Kinetic Theory of the Electromagnetic Drift Modes Driven by Pressure Gradients

W. Horton and J.E. Sedlak
Institute for Fusion Studies
University of Texas at Austin
Austin, Texas 78712

and

Duk-In Choi and B.G. Hong
Korea Advanced Institute
of Science and Technology
Chongyangni, Seoul, Korea

Abstract

Kinetic equations for the electromagnetic drift modes are derived and analyzed for the stability of tokamaks in the local approximation. In the dissipationless, hydrodynamic limit the fifth order polynomial dispersion relation previously studied is recovered. The kinetic velocity space integrals in the ion dynamics are shown to modify the five principal modes of oscillation and their polarizations. It is shown that in kinetic stability theory the critical plasma pressure defined in magnetohydrodynamic theory determines a transition from microinstability to macroinstability.

I. Introduction

In the low pressure plasma where beta is less than the square of the inverse aspect ratio of the system, the drift wave dispersion relation is a cubic polynomial describing the coupling of the electrostatic ion-acoustic oscillations with the $\underset{\sim}{E}\times\underset{\sim}{B}$ convection of the density and the ion pressure. For moderate to high plasma pressures these oscillations develop an electromagnetic component which couples them to the two low frequency magnetohydrodynamic ($E_{\parallel}=0$) branches of oscillations. The full linear electromagnetic description of the small amplitude oscillations of the system is given by a fifth order polynomial dispersion relation. An analysis of the five brances of oscillations $\omega_{\alpha}(k)$ with $\alpha=1,2,\ldots 5$ and their polarization is given by Horton et al.[1] as a function of plasma pressure $\beta=8\pi p/B^2$ and the inverse aspect ratio parameter $\varepsilon_n=r_n/R$. Here r_n is the radial scale length of the density gradient and R is the major radius of the toroidal plasma. In the work of Horton et al.[1] the two component hydrodynamic approximation is used for the plasma dynamics.

Here we derive and analyze the kinetic electromagnetic drift wave equations in the local approximation. The 3×3 matrix for the coupling of the electrostatic field, the inductive parallel vector potential and the parallel component of the magnetic field is derived with fully kinetic ion response functions. The 3×3 matrix is symmetric with complex elements involving generalized plasma dispersion functions.

From numerical studies and analytic approximations the problem of the transition from small scale electrostatic-like instability below β_c to MHD-like global instability above β_c is analyzed. In this study we neglect the effects of the dissipative electron response and the details of the toroidal mode ballooning structure. Dropping electron dissipation implies that the instabilities are driven purely by the ion and electron pressure gradients in the locally unfavorable magnetic curvature on the outside of the torus. The studies of Cheng[2] and Itoh et al.[3] include the solution of the surface eigenvalue problem in the ballooning approximation and the effect of trapped particles. Their studies neglect the important role in the pressure gradient driven modes of the perturbation in the strength of the magnetic field. The studies by Rewoldt et al.[4] include the perturbation to the strength of the magnetic field in a complicated numerical analysis of the stability problem. The high beta universal drift wave branch is studied by Hastings and McCune[5] for arbitrary β including the shear Alfven wave and the compressional component of $\delta \underset{\sim}{B}$. For $\eta_e=0$ they report stability for $\beta \geqslant 7\%$, but for $\eta_e>0$ the system remains unstable to β of order unity.

The kinetic theory stability analysis presented here extends the previous results of Ref. 1 giving the correct Vlasov response functions for modes with perpendicular wavelengths comparable to the ion gyroradius while including the complete description of the grad-B and curvature drift velocity resonance with the phase velocity. The fluid description is recovered by a double expansion in small ion gyroradius and small drift velocity. From the expansions given here and from the numerical examples the domain of validity of the fluid theory is clarified. Even in the regime of fluid theory the kinetic description removes the complex conjugate pair symmetry of the unstable fluid roots due to the analytic continuation of the response functions and the influence of their branch cut in the lower half ω-plane. The mathematical properties and algorithms for evaluating the guiding center response functions are given in Ref. 6.

II. Formulation

We use a representation[1] of the electric field

$$\underset{\sim}{E} = -\nabla\varphi - \nabla\times(a\hat{b}) - \frac{1}{c}\frac{\partial A_{\|}}{\partial t}\hat{b} \tag{1}$$

where $(\varphi, a, A_{\|})$ are the three components of potential and $\hat{b}$ is the local unit vector along $\underset{\sim}{B}$, $\hat{b} = \underset{\sim}{B}/B$. From the Faraday's law of $\frac{\partial}{\partial t}\delta\underset{\sim}{B} = -c\nabla\times\underset{\sim}{E}$ we have

$$\delta\underset{\sim}{B} = \hat{b}\frac{c}{i\omega}\nabla_{\perp}^{2}a + \nabla A_{\|}\times\hat{b} \equiv \delta B_{\|}\hat{b} + \delta\underset{\sim}{B}_{\perp} \tag{2}$$

where the time dependence of the perturbations is $\exp(-i\omega t)$.

Introducing the local coordinate system with the unit vectors of $(\hat{e}_x, \hat{e}_{\vartheta}, \hat{b})$ where $\hat{e}_x$ is the local radial unit vector and $\hat{e}_{\vartheta} = \hat{b}\times\hat{e}_x$, we obtain from the Ampere's law of $\frac{4\pi}{c}\delta\underset{\sim}{J} = \nabla\times\delta\underset{\sim}{B}$, the parallel component Ampere's law

$$\frac{4\pi}{c}\delta J_{\|} = \frac{4\pi}{c}\delta\underset{\sim}{J}\cdot\hat{b} = -\nabla_{\perp}^{2}A_{\|} \tag{3}$$

and the radial component Ampere's law

$$\frac{4\pi}{c}\delta J_x = \frac{4\pi}{c}\delta\underset{\sim}{J}\cdot\hat{e}_x = (\hat{e}_{\vartheta}\cdot\nabla)\delta B_{\|} \tag{4}$$

In the reductions leading to Eqs. (2)-(4), subdominant contributions are dropped.

In addition to Eqs. (3) and (4) the condition of quasineutrality

$$\sum_j \delta\rho_j = 0 \tag{5}$$

with $\delta\rho_j$ the perturbed charge density of j-species, $\delta\rho_j = e_j \delta n_j$, constitute the three mode equations of the electromagnetic fields. It is shown to be convenient to introduce the field ψ defined through the expression as

$$\frac{\partial\psi}{\partial s} = i \frac{\omega}{c} A_{\parallel} = \hat{b}\cdot\nabla\psi \tag{6}$$

so that $\underset{\sim}{E}_{\parallel} = -\hat{b}\cdot\nabla(\varphi-\psi)$. The coupled mode equations are obtained from Eqs. (3), (4) and (5) when we express the perturbed parallel and radial currents $\delta J_{\parallel}$ and δJ_x and the perturbed charge density $\delta\rho_j$ in terms of the field quantities $(\varphi, \psi, \delta B_{\parallel})$. The calculations of these perturbed quantities including the kinetic effects require the solutions of the gyrokinetic equations. In this respect, we utilize, with minor changes, the formulations developed by Antonsen et al.[7] and also by Tang et al.[8]

The solution of the gyrokinetic equation f_j is written as

$$f_j = -\frac{e_j}{T_j} \varphi F_j + g_j \exp(iL_j) \tag{7}$$

with

$$L_j = \underset{\sim}{k}\cdot\underset{\sim}{v}\times\hat{b}/\Omega_j$$

where $\Omega_j = e_j B/m_j c$. The nonadiabatic part of the distribution g_j satisfies

$$[v_\parallel \frac{\partial}{\partial s} - i(\omega-\omega_{Dj})]g_j$$

$$= - iF_j(\omega-\omega_{*tj}) \; [\frac{e_j}{T_j} (\varphi - \frac{v_\parallel}{c} A_\parallel)J_0 + \frac{a_j}{b_j} \frac{\delta B_\parallel}{B} J_1] \tag{8}$$

with the definitions of (j suppressed)

$$\omega_{*t} = \omega_*(1- \frac{3}{2}\eta + \eta \frac{mv^2}{2T})$$

$$\omega_D = \underset{\sim}{k}\cdot\hat{b}\times(\mu\nabla B+v_\parallel^2\hat{b}\cdot\nabla\hat{b})/\Omega$$

$$a = k_\perp v_\perp/\Omega, \qquad b = k_\perp^2 T/m\Omega^2, \qquad \mu = v^2{}_\perp/2B$$

$$\omega_* = \frac{cT}{eB} \underset{\sim}{k}_\perp\cdot\hat{b}\times\nabla\ell n\ n, \qquad \eta = \frac{d\ \ell n\ T}{d\ \ell n\ n} . \tag{9}$$

The modes we are interested in are the electromagnetic drift modes whose frequencies are bounded between the transit frequencies of the electrons and the ions. The frequencies are also assumed to be smaller than the electron bounce frequency to retain the trapped electron effects. That is

$$\omega_{te} = v_e/L_c > \omega_{be} > \omega > \omega_{ti} = v_i/L_c$$

where L_c is the connection length and v_j is the thermal velocity of the j–th species.

1. Electrons

The solutions of Eq. (8) for electrons are obtained in the lowest order of the parameters $\omega L_c/v_e$ and $k_\perp \rho_e$. Depending on whether we have the passing electrons or the trapped electrons, we have the following solutions.

a. Passing electrons:

$$\frac{1}{2}(g_+ + g_-)_e^p = -F_e\left(1 - \frac{\omega_{*te}}{\omega}\right)\psi \qquad (10)$$

where subscripts ± indicate the sign of $v_\parallel$ and superscript p indicates the passing particles. The field ψ is the normalized quantity differing from the ψ introduced in Eq. (6) by the factor e/T_e. Unless indicated otherwise, the fields of φ and ψ appearing in the following are all normalized to e/T_e.

b. Trapped electrons:

$$\frac{1}{2}(g_+ + g_-)_e^t = -F_e\left[\left(1 - \frac{\omega_{*te}}{\omega}\right)\psi + Y\right] \qquad (11)$$

where the bounce average field quantity Y is given by

$$Y = \left(\frac{\omega - \omega_{*te}}{\omega - \bar{\omega}_{De}}\right)\bar{X}$$

and X is, in turn, given by

$$X = [\varphi - (1 - \frac{\omega_{De}}{\omega})\psi - \frac{v_\perp^2}{v_e^2} \frac{\delta B_\parallel}{B}] \quad . \tag{12}$$

The top bar denotes the bounce average defined as

$$\overline{A} = \oint \frac{ds}{|v_\parallel|} A/\oint \frac{ds}{|v_\parallel|} \quad . \tag{13}$$

2. Ions

For ions we have all passing particles and expanding in powers of $v_i/\omega L_c$ we obtain

$$\frac{1}{2} (g_+ + g_-)_i = F_i(\frac{\omega-\omega_{*ti}}{\omega-\omega_{Di}}) (1-\sigma^2)^{-1} \cdot [\tau\varphi J_0 + \frac{a_i}{b_i} \frac{\delta B_\parallel}{B} J_1 + \frac{J_0|v_\parallel|^2}{\omega(\omega-\omega_{Di})} \frac{\partial^2}{\partial s^2} \tau\psi], \tag{14}$$

where $\tau = T_e/T_i$ and

$$\sigma = \frac{i|v_\parallel|}{(\omega-\omega_{Di})} \frac{\partial}{\partial s} \quad . \tag{15}$$

3. Quasi-neutrality

From Eqs. (7), (10), and (11) we obtain the electron perturbed density δn_e of

$$\frac{\delta n_e}{n_o} = \varphi - \left[\left(1 - \frac{\omega_{*e}}{\omega}\right)\psi + \sqrt{2\varepsilon}\ \langle Y\rangle_{tr}\right] \tag{16}$$

where we defined a trapped particle operator $\langle\ldots\rangle_{tr}$ as the velocity integration over the trapped particle region weighted by the normalized Maxwellian $\frac{1}{n_o} F_e$

$$\sqrt{2\varepsilon}\ \langle g(\underset{\sim}{v})\rangle_{tr} = \frac{1}{n_o}\int_{tr} d\underset{\sim}{v}\ F_e\ g(\underset{\sim}{v}) \quad . \tag{17}$$

The ion density perturbation δn_i is obtained from Eqs. (7) and (14) as

$$\frac{\delta n_i}{n_o} = \left(\tau P - P_3 \frac{c_s^2}{\omega^2}\frac{\partial^2}{\partial s^2}\right)\varphi + P_2 \frac{c_s^2}{\omega^2}\ \frac{\partial^2 \psi}{\partial s^2} + \left(Q - \frac{Q_3}{\tau}\frac{c_s^2}{\omega^2}\frac{\partial^2}{\partial s^2}\right)\frac{\delta B_\parallel}{B} \tag{18}$$

where c_s is the ion sound velocity $(T_e/m_i)^{1/2}$. The quasi-neutrality of $\delta n_e = \delta n_i$ then gives one mode equation of

$$\left[-1+\tau(P-1) - \frac{c_s^2}{\omega^2} P_3 \frac{\partial^2}{\partial s^2}\right]\varphi + \left[\left(1 - \frac{\omega_{*e}}{\omega}\right) + P_2 \frac{c_s^2}{\omega^2}\frac{\partial^2}{\partial s^2}\right]\psi$$

$$+\left(Q - \frac{Q_3}{\tau}\frac{c_s^2}{\omega^2}\frac{\partial^2}{\partial s^2}\right)\frac{\delta B_\parallel}{B} + \sqrt{2\varepsilon}\ \ \langle Y\rangle_{tr} = 0 \quad . \tag{19}$$

The ion kinetic integrals of P and Q's including the ion drift resonances are given as

$$P = <(\frac{\omega-\omega_{*ti}}{\omega-\omega_{Di}}) J_0^2> \ , \quad P_j = < \frac{\omega^{j-1}(\omega-\omega_{*ti})}{(\omega-\omega_{Di})^j} \ \frac{m_i}{T_i} \ v_\parallel^2 \ J_o^2> \tag{20}$$

$$Q = <(\frac{\omega-\omega_{*ti}}{\omega-\omega_{Di}})(\frac{1}{b_i} \frac{m_i}{T_i})^{1/2} \ v_\perp J_0 J_1> \ ,$$

and

$$Q_j = < \frac{\omega^{j-1}(\omega-\omega_{*ti})}{(\omega-\omega_{Di})^j} \ \frac{1}{\sqrt{b}} \ (\frac{m_i}{T_i})^{3/2} v_\perp v_\parallel^2 J_0 J_1> \tag{21}$$

where $(j = 2,3)$ and < > is defined as the average over the Maxwellian velocity distribution

$$<A> = \frac{1}{n_0} \int d\underset{\sim}{v} \ F_i \ A \tag{22}$$

The analytic properties, small and large argument expansions and the numerical evaluation of the guiding center dispersion functions are given in terms of $G_j^{FLR}(\omega,a,b)$ by Similon et al.[6] The guiding center dispersion function has a branch cut from $\omega = 0$ to $\omega = -i\infty$.

4. Parallel Component Ampere's Law

The parallel derivative ($\partial/\partial s$) of the perturbed parallel current

$$\delta J_{\parallel j} = e_j \int d\underset{\sim}{v}\; v_\parallel f_j \tag{23}$$

is conveniently computed directly from the kinetic equation (8) by operating $e_j \int d\underset{\sim}{v}\, \exp(iL)$ and we obtain

$$\frac{\partial}{\partial s}\, \delta J_{\parallel j} = i e_j \int d\underset{\sim}{v}\; J_0 \frac{1}{2} (g_+ + g_-)_j\; (\omega - \omega_{Dj})$$

$$-ie_j \int d\underset{\sim}{v}\; F_j\; J_0\; (\omega - \omega_{*tj})\; \left(\frac{e_i}{T_j}\, \varphi J_0 + \frac{a_j}{b_j}\, \frac{\delta B_\parallel}{B}\, J_1\right) \tag{24}$$

(Here φ is not normalized.)

For the electron contribution using Eqs. (10) and (11) in Eq. (24) we obtain

$$\frac{\partial}{\partial s}\, \delta J_{\parallel e} = i\omega n_0 e\; \{-(1 - \frac{\omega_{*e}}{\omega})\varphi + \sqrt{2\varepsilon}\; <(1 - \frac{\omega_{De}}{\omega})Y>_{tr}$$

$$+\left[(1 - \frac{\omega_{*e}}{\omega}) - (\frac{\omega_\kappa^e + \omega_{\nabla B}^e}{\omega})(1 - \frac{\omega_{*pe}}{\omega}) \right]\psi + (1 - \frac{\omega_{*pe}}{\omega})\; \frac{\delta B_\parallel}{B}\} \tag{25}$$

where we introduced the definitions of

$$\omega_{*pj} = \omega_{*j}(1+\eta_j), \qquad \omega_\kappa^j = \frac{cT_j}{e_j B}\, \hat{b}\times\hat{b}\cdot\nabla\hat{b}\cdot\underset{\sim}{k}_\perp\;, \qquad \omega_{\nabla B}^j = \frac{cT_j}{e_j B}\, \hat{b}\times\frac{\nabla B}{B}\cdot\underset{\sim}{k}_\perp\;. \tag{26}$$

For the computation of the ion contribution to the perturbed current, an identity can be derived from the solution of the ion kinetic equation, Eq. (14). Expanding $(1-\sigma^2)^{-1}$ and rearranging it we have an identity in the form

$$i\ e \int d\underset{\sim}{v}\ J_0 \frac{1}{2} (g_+ + g_-)_i(\omega - \omega_{Di}) - i\ e \int d\underset{\sim}{v}\ F_i\ J_0\ (\omega - \omega_{*ti})\left(J_0 \tau\varphi + \frac{a}{b} J_1 \frac{\delta B_\parallel}{B}\right)$$

$$= i\ e \int d\underset{\sim}{v}\ F_i\ J_0\ \left(1 - \frac{\omega_{*ti}}{\omega}\right) \frac{v_\parallel^2}{(\omega-\omega_{Di})} (1 - \sigma^2)^{-1}$$

$$\cdot\left(J_0^2 \frac{\partial^2}{\partial s^2} \tau\psi - J_0 \frac{\omega}{(\omega-\omega_{Di})} \frac{\partial^2}{\partial s^2} \tau\varphi - J_1 \frac{a}{b} \frac{\omega}{(\omega-\omega_{Di})} \frac{\partial^2}{\partial s^2} \frac{\delta B_\parallel}{B}\right) \qquad (27)$$

The left hand side of Eq. (27) is $\frac{\partial}{\partial s} \delta J_{\parallel i}$ by Eq. (24) and thus we obtain in the lowest order the ion contribution of

$$\frac{\partial}{\partial s} \delta J_{\parallel i} = i\omega n_0 e \frac{c_s^2}{\omega^2} \frac{\partial^2}{\partial s^2} \left(P_1\psi - P_2\varphi - \frac{Q_2}{\tau} \frac{\delta B_\parallel}{B}\right) \qquad (28)$$

Taking $\partial/\partial s$ of the parallel Ampere's law Eq. (3) and making use of Eq. (6), we have the parallel Ampere's law in the form of

$$\frac{\partial}{\partial s} \delta J_\parallel = -\frac{c}{4\pi} \frac{\partial}{\partial s} \nabla_\perp^2 A_\parallel = i \frac{c^2}{4\pi\omega} \frac{\partial}{\partial s} \nabla_\perp^2 \frac{\partial}{\partial s} \psi \qquad (29)$$

and making use of Eqs. (25) and (28) in the left hand side of Eq. (29) we obtain

$$\frac{\rho^2 v_A^2}{\omega^2} \frac{\partial}{\partial s} \nabla_\perp^2 \frac{\partial}{\partial s} \psi = -\left[\left(1 - \frac{\omega_{*e}}{\omega}\right) + P_2 \frac{c_s^2}{\omega^2} \frac{\partial^2}{\partial s^2}\right]\varphi + \sqrt{2\varepsilon} \left\langle\left(1 - \frac{\omega_{De}}{\omega}\right) Y\right\rangle_{tr}$$

$$+ \left[\left(1-\frac{\omega_{*e}}{\omega}\right) - \left(1-\frac{\omega_{*pe}}{\omega}\right)\left(\frac{\omega_\kappa^e+\omega_{\nabla B}^e}{\omega}\right) + P\,\frac{c_s^2}{\omega^2}\frac{\partial^2}{\partial s^2}\right]\psi$$

$$+\left[\left(1-\frac{\omega_{*pe}}{\omega}\right) - \frac{Q_2}{\tau}\frac{c_s^2}{\omega^2}\frac{\partial^2}{\partial s^2}\right]\frac{\delta B_\parallel}{B} \tag{30}$$

where the Alfvèn velocity $v_A = (B^2/4\pi n_0 m_i)^{1/2}$ is defined.

5. <u>Radial Component Ampere's Law</u>

Since the radial component perturbed current δJ_x can be computed as[4,5]

$$\delta J_x = -i\,\frac{k_\vartheta}{k_\perp}\sum_j e_j \int d\underset{\sim}{v}\,\frac{1}{2}(g_+ + g_-)_j\; v_\perp J_1 \tag{31}$$

we obtain the electron contribution by making use of Eqs. (10) and (11) into Eq. (31) as

$$\delta J_x^e = \frac{ik_\vartheta n_0 e T_e}{m_i\Omega_i}\left[\left(1-\frac{\omega_{*pe}}{\omega}\right)\psi + \sqrt{2\varepsilon}\,\langle Y\rangle_{tr}\right] \tag{32}$$

and also by making use of the ion solution Eq. (14) into Eq. (31), we get the ion contribution to the perturbed radial current

$$\delta J_x^i = -\frac{ik_\vartheta n_0 e T_i}{m_i\Omega_i}\left[\left(\tau Q - Q_3\frac{c_s^2}{\omega^2}\frac{\partial^2}{\partial s^2}\right)\varphi + Q_2\frac{c_s^2}{\omega^2}\frac{\partial^2}{\partial s^2}\psi + \left(R - \frac{R_3}{\tau}\frac{c_s^2}{\omega^2}\frac{\partial^2}{\partial s^2}\right)\frac{\delta B_\parallel}{B}\right]. \tag{33}$$

Putting Eqs. (31)-(33) into the radial component Ampere's laws of Eq. (4), we obtain

$$\frac{\delta B_{\|}}{B} = \frac{\beta_e}{2} \left[\left(1 - \frac{\omega_{*pe}}{\omega}\right)\psi + \sqrt{2\varepsilon} \left< \frac{m_e v_\perp^2}{2T_e} Y \right>_{tr} \right]$$

$$- \frac{\beta_i}{2} \left[\left(\tau Q - Q_3 \frac{c_s^2}{\omega^2} \frac{\partial^2}{\partial s^2}\right)\varphi + Q_2 \frac{c_s^2}{\omega^2} \frac{\partial^2 \psi}{\partial s^2} + \left(R - \frac{R_3}{\tau} \frac{c_s^2}{\omega^2} \frac{\partial^2}{\partial s^2}\right) \frac{\delta B_{\|}}{B} \right]. \qquad (34)$$

We defined β_j as $\beta_j = 8\pi n_0 T_j / B^2$ and other ion kinetic integrals R and R_3 as

$$R \doteq \left< \left(\frac{\omega-\omega_{*ti}}{\omega-\omega_{Di}}\right) \frac{1}{b} \frac{m_i}{T_i} v_\perp^2 J_1^2 \right> \qquad (35)$$

and

$$R_3 = \left< \frac{\omega^2(\omega-\omega_{*ti})}{(\omega-\omega_{Di})^3} \frac{1}{b} \left(\frac{m_i}{T_i}\right)^2 v_\perp^2 v_\|^2 J_1^2 \right> .$$

The three equations, quasi-neutrality Eq. (19), parallel Ampere's law Eq. (30), and the radial Ampere's law Eq. (34), constitute the coupled mode equations for the fields φ, ψ and $\delta B_{\|}$.

III. Kinetic Dispersion Relation of Electromagnetic Drift Waves

The three mode equations derived in Sec. II are in the form of the coupled differential equations exhibiting the non-local ballooning nature of the modes. In this section we assume that the axial problem of the mode structure is solved and that the modes are localized in the bad curvature region as the result. We also neglect the trapped electron effect, not because it is unimportant but rather for the purpose of the simplification and the additional effect can be studied in a separate study. Thus we obtain the local dispersion relation by letting $\partial/\partial s \rightarrow ik_{\parallel}$ and $\nabla_{\perp}^2 \rightarrow -k_{\perp}^2$ in the three mode equations of the quasineutrality Eq. (19), parallel Ampere's law Eq. (30) and the radial Ampere's law Eq. (34)

$$a\varphi + b\psi + c\delta B = 0 \qquad (36)$$

$$b\varphi + d\psi + e\delta B = 0 \qquad (37)$$

$$c\varphi + e\psi + f\delta B = 0 \qquad (38)$$

or in the matrix form

$$MX = 0 \qquad (39)$$

with the complex symmetric matrix

$$M = \begin{bmatrix} a & b & c \\ b & d & e \\ c & e & f \end{bmatrix} \qquad (40)$$

and the field quantities vectorized as

$$X = \begin{matrix} \varphi \\ \psi \\ \delta B \end{matrix} \quad . \qquad (41)$$

Here we have introduced a short hand notation for the normalized parallel magnetic field fluctuation $\delta B = \delta B_{\parallel}/B$. With the definitions of $\omega_s = k_{\parallel} c_s$ and $\omega_A = k_{\parallel} v_A$, we have the formulas for the matrix elements of M in terms of the kinetic integrals as

$$a = -1 + \tau(P-1) + \frac{\omega_s^2}{\omega^2} P_3 \;, \quad b = 1 - \frac{\omega_{*e}}{\omega} - \frac{\omega_s^2}{\omega^2} P_2 \;,$$

$$c = Q + \frac{\omega_s^2}{\omega^2} \frac{Q_3}{\tau} \;, \quad d = \frac{k_\perp^2 \rho^2 \omega_A^2}{\omega^2} - (1 - \frac{\omega_{*e}}{\omega}) + (1 - \frac{\omega_{*pe}}{\omega})(\frac{\omega_\kappa^e + \omega_{\nabla B}^e}{\omega}) + \frac{\omega_s^2}{\omega^2} P_1$$

$$e = - (1 - \frac{\omega_{*pe}}{\omega}) - \frac{\omega_s^2}{\omega^2} \frac{Q_2}{\tau}, \quad f = \frac{2}{\beta_e} + \frac{1}{\tau} (R + \frac{\omega_s^2}{\omega^2} \frac{R_3}{\tau}) \tag{42}$$

where the cross-field ion inertial scale radius ρ is defined by $\rho = c(m_i T_e)^{1/2}/eB$.

We now eliminate δB in favor of φ and ψ from Eq. (39) to reduce the system to a 2×2 matrix. solving for δB from the radial component of Amperes law Eq. (38) and substituting into the quasineutrality Eq. (36) and the parallel Ampere's law Eq. (37), we have $\delta B = -(c\varphi + e\psi)/f$ or

$$\frac{\delta B_{\parallel}}{B} = \frac{\beta_e}{2} \frac{[-(Q + \frac{\omega_s^2}{\omega^2} \frac{Q_3}{\tau})\varphi + (1 - \frac{\omega_{*pe}}{\omega} + \frac{\omega_s^2}{\omega^2} \frac{Q_2}{\tau})\psi]}{[1 + \frac{\beta_i}{2} (R + \frac{\omega_s^2}{\omega^2} \frac{R_3}{\tau})]} \tag{43}$$

and substituting Eq. (43) into Eq. (36) we get the new form for quasi-neutrality as

$$(a - \frac{c^2}{f})\varphi + (b - \frac{ce}{f})\psi = 0$$

or

$$A(\omega)\varphi = B(\omega)\psi \qquad (44)$$

where the A and B are given by

$$A(\omega) = \omega^3\{[1-\tau(P-1) - \frac{\omega_s^2}{\omega^2} P_3] + \frac{\beta_e}{2} \frac{(Q+ \frac{\omega_s^2}{\omega^2} \frac{Q_3}{\tau})^2}{[1 + \frac{\beta_i}{2} (R+ \frac{\omega_s^2}{\omega^2} \frac{R_3}{\tau})]}\}$$

and

$$B(\omega) = \omega^3\{(1 - \frac{\omega_{*e}}{\omega} - \frac{\omega_s^2}{\omega^2} P_2) + \frac{\beta_e}{2} \frac{(Q + \frac{\omega_s^2}{\omega^2} \frac{Q_3}{\tau})(1 - \frac{\omega_{*pe}}{\omega} + \frac{\omega_s^2}{\omega^2} \frac{Q_2}{\tau})}{[1 + \frac{\beta_i}{2} (R + \frac{\omega_s^2}{\omega^2} \frac{R_3}{\tau})]}\} .$$

Similarly, we obtain for the parallel component of Ampere's law the formulas

$$(b - \frac{ce}{f})\varphi + (d - \frac{e^2}{f})\psi = 0$$

or

$$B(\omega)\varphi = K(\omega)\psi \tag{45}$$

where K is given by

$$K(\omega) = \omega^3 \left(\frac{e^2}{f} - d\right)$$

$$= \omega^3\left[\left(1-\frac{\omega_{*e}}{\omega}\right) - \frac{k_\perp^2\rho^2\omega_A^2}{\omega^2} - \left(1-\frac{\omega_{*pe}}{\omega}\right)\left(\frac{\omega_\kappa^e+\omega_{\nabla B}^e}{\omega}\right) - \frac{\omega_s^2}{\omega^2} P_1\right]$$

$$+ \frac{\beta_e}{2} \frac{\left(1-\frac{\omega_{*pe}}{\omega} + \frac{\omega_s^2}{\omega^2}\frac{Q_2}{\tau}\right)^2}{\left[1+\frac{\beta_i}{2}\left(R+\frac{\omega_s^2}{\omega^2}\frac{R_3}{\tau}\right)\right]} . \tag{46}$$

Note that the reduced 2×2 matrix from Eqs. (44) and (45) is also symmetric. As will be discussed below, it turns out to be more convenient to use an alternative form of Eq. (45). Namely, by taking the difference between Eqs. (44) and (45) we obtain

$$C(\omega)\varphi = D(\omega)\psi \tag{47}$$

with

$$C(\omega) = (A-B)/\omega$$

$$= \omega^2\{[\frac{\omega_{*e}}{\omega} - \tau(P-1) + \frac{\omega_s^2}{\omega^2}(P_2-P_3)]$$

$$+ \frac{\beta_e}{2} \cdot \frac{(Q + \frac{\omega_s^2}{\omega^2}\frac{Q_3}{\tau})[Q-(1-\frac{\omega_{*pe}}{\omega}) + \frac{\omega_s^2}{\tau\omega^2}(Q_3-Q_2)]}{[1+\frac{\beta_i}{2}(R+\frac{\omega_s^2}{\omega^2}\frac{R_3}{\tau})]}\}$$

and

$$D(\omega) = (B-K)/\omega$$

$$= \omega^2\{[\frac{k_\perp^2\rho^2\omega_A^2}{\omega^2} + (1-\frac{\omega_{*pe}}{\omega})(\frac{\omega_\kappa^e+\omega_{\nabla B}^e}{\omega}) + \frac{\omega_s^2}{\omega^2}(P_1-P_2)]$$

$$+ \frac{\beta_e}{2}\frac{(1-\frac{\omega_{*pe}}{\omega} + \frac{\omega_s^2}{\tau\omega^2}Q_2)[Q-(1-\frac{\omega_{*pe}}{\omega}) + \frac{\omega_s^2}{\tau\omega^2}(Q_3-Q_2)]}{[1+\frac{\beta_i}{2}(R+\frac{\omega_s^2}{\omega^2}\frac{R_3}{\tau})]}\} \quad . \qquad (48)$$

Any two of the three equations thus formed from the quasineutrality equation (44), the parallel Ampere's law equation (45) or the combined equation (47) can be taken as the fundamental two coupled equations for determining the two fields φ and ψ. However, it is demonstrated in Ref. 1 that Eq. (47) is convenient and useful in analytic studies of the fields and, in particular, the polarizations and the case of the magnetohydrohynamics (MHD) like modes are readily obtained using $C\varphi=D\psi$. To derive the analytic approximations to the dispersion relations we first consider the various ion kinetic integrals in the fluid limit. Using the superscript f to denote the fluid limit of the kinetic response functions, we find that

$$P^f = (1 - \frac{\omega_{*i}}{\omega}) + (1 - \frac{\omega_{*pi}}{\omega}) (\frac{\omega_\kappa^i + \omega_{\nabla B}^i}{\omega} - b_i)$$

(The b_i here is $k_\perp^2 T_i/m_i \Omega_i^2 = k_\perp^2 \rho_i^2$ defined in Eq. (9) and not to be confused with b defined in Eq. (42).)

$$P_1^f = P_2^f = P_3^f = Q^f = 1 - \frac{\omega_{*pi}}{\omega}$$

$$Q_2^f = Q_3^f = \frac{1}{2} R^f = 1 - \frac{\omega_{*i}}{\omega} (1+2\eta_i) \quad . \qquad (49)$$

$$\frac{1}{2} R_3^f = 1 - \frac{\omega_{*i}}{\omega} (1+3\eta_i)$$

In the fluid limit Eqs. (48) and (49) reduce to

$$C^f = \omega^2 [\tau(1- \frac{\omega_{*pi}}{\omega})(b_i - \frac{\omega_\kappa^i + \omega_{\nabla B}^i}{\omega}) + \frac{\beta_e}{2} (1- \frac{\omega_{*pi}}{\omega}) (\frac{\omega_{*pe} - \omega_{*pi}}{\omega})]$$

$$= (\omega - \omega_{*pi})(\omega k_\perp^2 \rho^2 + 2\omega_\kappa^e)$$

and

$$D^f = \omega^2\left[\frac{k_\perp^2\rho^2\omega_A^2}{\omega^2} + \left(1-\frac{\omega_{*pe}}{\omega}\right)\left(\frac{\omega_\kappa^e + \omega_{\nabla B}^e}{\omega}\right) + \frac{\beta_e}{2}\left(1-\frac{\omega_{*pe}}{\omega}\right)\left(\frac{\omega_{*pe}-\omega_{*pi}}{\omega}\right)\right]$$

$$= k_\perp^2\rho^2\omega_A^2 + 2\omega_\kappa^e\,(\omega-\omega_{*pe}) \qquad (50)$$

where we made use of the identities derived in Ref. 1 in the form of

$$\frac{\beta_e}{2}(\omega_{*pe} - \omega_{*pi}) + \omega_{\nabla B}^e = \omega_\kappa^e$$

and

$$\frac{\beta_e}{2}(\omega_{*pe} - \omega_{*pi}) - \tau\omega_{\nabla B}^i = -\tau\omega_\kappa^i \qquad (51)$$

to eliminate the $\omega_{\nabla B}^e$ and $\omega_{\nabla B}^i$ drifts. With the introduction of the polarization as $\alpha = \psi/\varphi$, we have from Eqs. (44) and (47) the polarization relation

$$\alpha(\omega) = \frac{A(\omega)}{B(\omega)} = \frac{C(\omega)}{D(\omega)} \qquad (52)$$

which can be viewed as the kinetic dispersion relationship. In the fluid limit of C and D of Eq. (50) together with the MHD-like requirement of $E_\parallel \simeq 0$ or $\varphi \simeq \psi$, that is $\alpha \simeq 1$, we obtain

$$(\omega-\omega_{*pi})(\omega k_\perp^2\rho^2+2\omega_\kappa^e) = k_\perp^2\rho^2\omega_A^2+2\omega^e{}_\kappa(\omega-\omega_{*pe})$$

or

$$\omega^2 - \omega_{*pi}\omega + \frac{2\omega_\kappa^e}{k_\perp^2\rho^2}(\omega_{*pe}-\omega_{*pi})-\omega_A^2 = 0 \qquad (53)$$

giving the two MHD modes

$$\omega = \frac{1}{2}\omega_{*pi} \pm i\left(\frac{2\omega_\kappa^e}{k_\perp^2\rho^2}(\omega_{*pe}-\omega_{*pi})-\omega_A^2+\frac{\omega_{*pi}^2}{4}\right)^{1/2}, \qquad (54)$$

which in the dimensionless variables defined in Ref. 1 becomes

$$= -\frac{k}{2}(1+\eta_i) \pm i\left[\frac{k^2}{k_\perp^2}\gamma_m^2 - \frac{k^2}{4}(1+\eta_i)^2-\omega_A^2\right]^{1/2}$$

for the well known MHD branch modes. Following Ref. 1, we define the dimensionless MHD growth rate γ_m by

$$\gamma_m^2 = 2\varepsilon_n\left[1+\eta_e+\frac{1+\eta_i}{\tau}\right]$$

in terms of ε_n, η_e, η_i, τ. All frequencies are measured in units of c_s/r_n and the cross-field wavenumber $\underset{\sim}{k}_\perp$ in units of $\rho = c(m_iT_e)^{1/2}/eB$. The dimensionless frequencies are, then, given by

$$\omega_{*e} = k, \quad \omega_{*pe} = k(1+\eta_e), \quad \omega_{*pi} = -\frac{k(1+\eta_i)}{\tau}, \quad \omega_\kappa^e = k\,\varepsilon_n, \quad \omega_\kappa^i = -\frac{k\varepsilon_n}{\tau}$$

$$\omega^e_{\nabla B} = k\varepsilon_n - \frac{\beta_e}{2}(\omega_{*pe}-\omega_{*pi}), \quad \omega^i_{\nabla B} = -\omega^e_{\nabla B}/\tau$$

$$\omega_s = \frac{\varepsilon_n}{q}, \quad \omega_A = \left(\frac{2}{\beta_e}\right)^{1/2}\frac{\varepsilon_n}{q} \tag{55}$$

and $\varepsilon_n = r_n/R$ with $\beta_j = 8\pi P_j/B^2$, and $b = \tau b_i = k^2$.

IV. Comparison with the Fluid Limit and the Numerical Solutions

Here we present some of the results of our numerical solutions of the kinetic dispersion relation for $\omega_\alpha(k)$ and give approximate analytic formulas that explain several features of the numerical results. The analytic results are obtained from the fluid limits of the response functions.

A. Analytic Results

The compressional component of the magnetic fluctuation in the regime $\omega^2 >> \omega_s^2$ and $\beta_i << 1$ reduces from Eq. (43) to

$$\delta B(\omega) = -\frac{\beta_e}{2}\left[Q(k,\omega) - \alpha\left(1 - \frac{\omega_{*pe}}{\omega}\right)\right]\varphi$$

where $\alpha = \psi/\varphi$ is given by Eq. (52). In the fluid limit with $Q \to Q^f$ the compressional component reduces to

$$\delta B^f = -\frac{\beta_e}{2}\left[1 - \frac{\omega_{*pi}}{\omega} - \alpha_k\left(1 - \frac{\omega_{*pe}}{\omega}\right)\right]\varphi$$

$$= - \frac{4\pi(\delta p_i^f + \delta p_e^f)}{B^2} \tag{56}$$

where the last formula follows from Eqs. (17) and (18) of Ref. 1.

Although small in absolute magnitude, the role of δB is essential in the stability analysis since taken with identities (51) the contributions of $\omega_{\nabla B}^{i,e}$ cancel from the dispersion relation. From Eq. (56) and the quasineutrality equation we find that the reduction of the dispersion relation to the pressure gradient driven modes introduces the effective growth rate parameter

$$\gamma(\alpha) = \{2\varepsilon_n[\frac{1+\eta_i}{\tau} + \alpha(1+\eta_e)]\}^{1/2} \tag{57}$$

where α describes the electrostatic to MHD transition of the modes. For the electrostatic and MHD limits we have, respectively,

$$\gamma_0 = \gamma(\alpha=0) = [2\varepsilon_n(1+\eta_i)/\tau]^{1/2} \tag{58}$$

as defined in the electrostatic studies of Refs. 9-11 and

$$\gamma_m = \gamma(\alpha=1) = \{2\varepsilon_n[(\frac{1+\eta_i}{\tau}) + (1+\eta_e)]\}^{1/2} \tag{59}$$

which is the MHD growth rate as defined after Eq. (54).

The kinetic formula for α is given in Eq. (52) and the fluid limit follows from formula (50). An alternative fluid limit follows from Eq. (45) with $\omega >> \omega_s$, ω_D and $\beta << 1$. We obtain from Eqs. (44), (45) and (46)

$$\alpha_k^f(\omega) = \frac{1}{1 - \frac{k_\perp^2 \rho^2 \omega_A^2}{\omega(\omega - \omega_{*e})}} \tag{60}$$

Along the unstable branch with $\omega \simeq i\gamma_m >> k$ the polarization is approximately

$$\alpha_k = \frac{1}{1+k^2\omega_A^2/\gamma_m^2} = \frac{1}{1+k^2\beta_c/\beta} \tag{61}$$

where $\gamma_m^2/\omega_A^2 = \beta/\beta_c$ with

$$\beta_c = \frac{\varepsilon_n(1 + \frac{1}{\tau})}{q^2(\frac{1+\eta_i}{\tau} + 1+\eta_e)} = \frac{\varepsilon_p}{q^2} \tag{62}$$

as given in Eq. (43) of Ref. 1. Formula (61) shows that there is a beta dependent transitional wavelength for the change from electrostatic to MHD-like polarization of the pressure gradient driven modes.

For short wavelengths such that

$$k > k_c = (\beta/\beta_c)^{1/2} \quad \Rightarrow \quad 0 < \alpha_k < \frac{1}{2}$$

the polarization is electrostatic, and for long wavelengths

$$k < k_c = (\beta/\beta_c)^{1/2} \quad \Rightarrow \quad \frac{1}{2} < \alpha_k < 1$$

the polarization is MHD-like. This variation of the polarization with k and β/β_c is verified by the numerical studies.

Following Refs. 1 and 9-11 we define the phase velocity of the toroidal electron drift wave as

$$u_k = \frac{1-2\varepsilon_n(1-\alpha)-k^2(1+\eta_i)/\tau}{1+k^2} \tag{63}$$

From the fluid limits derived in Sec. III we derive the transitional dispersion relation

$$\omega(\omega-\omega_{*e})[\omega(\omega-\omega_{*pi})+\gamma^2(\alpha)] - \omega_A^2(1+k^2)[\omega(\omega-ku_k) + \frac{k^2\gamma^2(\alpha)}{1+k^2}] = 0 \tag{64}$$

where $\gamma(\alpha)$ is given by Eq. (57) and u_k by Eq. (63). Equation (64) may also be derived from Eq. (35) in Ref. (1) with $\omega_s^2/\omega^2 \sim \beta << 1$ and $k \sim \varepsilon_n{}^{1/2}$. Equation (64) does not apply for $\omega \sim \omega_s$ nor $k \to 0$.

(i) Low Beta Regime

For low plasma pressure $\beta \sim \varepsilon_n^2$ the unstable mode is approximately electrostatic $(\alpha << 1)$. Taking into account the electromagnetic correction γ_m^2/ω_A^2 in Eq. (64) we obtain

$$\omega^2 - \omega k\tilde{u}_k + \frac{k^2\gamma^2(\alpha)}{1+k^2-\gamma_m^2/\omega_A^2} = 0 \tag{65}$$

where

$$\tilde{u}_k = \frac{1-2\varepsilon_n(1-\alpha)-k^2\frac{1+\eta_i}{\tau}-\gamma_m^2/\omega_A^2}{1+k^2-\gamma_m^2/\omega_A^2}$$

For $\beta \lesssim \varepsilon_n^2$ the unstable roots are given by $\omega^2-\omega k u_k+k^2\gamma_0^2/(1+k_0^2) = 0$ as derived in Horton, Choi and Tang[10] and studied with a nonlinear simulation by Brock and Horton.[11] The coupling to the Alfven wave lowers the phase velocity $\tilde{u}_k$ of the drift wave.

For higher $\beta \gtrsim \varepsilon_n^2$ we see from Eq. (65) that the fastest growing wavenumber $k=k_m(\beta,\eta_i,\varepsilon_n)$ is given by

$$k_m = \left[\frac{(1-2\varepsilon_n-\beta/\beta_c)}{(1+\eta_i)/\tau} \right]^{1/2} \tag{66}$$

where $\beta_c = \dfrac{\varepsilon_n(1+1/\tau)/q^2}{1+\eta_e+(1+\eta_i)/\tau}$ and $\gamma_{max} \simeq (2\varepsilon_n)^{1/2}$.

It is useful to exptrapolate the low beta formulas (65)-(66) to $\beta=\beta_c$ to compare with the high beta formulas. For $\beta \lesssim \beta_c$ and $k<k_c=(\beta/\beta_c)^{1/2}$ the polarization is $\alpha \simeq 1$ giving $\gamma(\alpha)\simeq\gamma_m$ and $k_m(\beta,\eta,\varepsilon_n) \to 0$. For $k = k_m \simeq 0$ the unstable root of Eq. (65) is

$$\gamma_k(\beta) = \frac{k\gamma_m}{(1+k_\perp^2-\beta/\beta_c)^{1/2}} \tag{67}$$

where $\beta/\beta_c = \gamma_m^2/\omega_A^2$. Thus, we find that from the low beta side

$$\lim_{\beta\to\beta_c} \gamma_k = \frac{k}{k_\perp}\gamma_m \tag{68}$$

which agrees with the MHD formula (54) valid for the high beta plasma.

(ii) Transitional Plasma Beta

In the transitional regime we may view Eq. (64) as giving the drift wave coupling corrections to the MHD dispersion relation (53). There are two principal physical effects modifying the MHD equations. There is the reduction in the electron pressure gradient contribution due to $\alpha<1$ and the modification of the line-bending stabilization due to the coupling of the shear Alfvèn wave ω_A with the drift wave ω_{*e}.

For the effect of $\alpha < 1$ we find that the modification to the MHD growth rate is given by

$$\tilde{\gamma}_m = \left\{2\varepsilon_n\left[\frac{1+\eta_i}{\tau} + \frac{1+\eta_e}{1+k^2\beta_c/\beta}\right]\right\}^{1/2} \tag{69}$$

obtained from Eqs. (57) and (61).

The modified growth rate $\tilde{\gamma}_m$ reduces to the classical result γ_m given in Eq. (54) for $k<(\beta/\beta_c)^{1/2}$. For shorter wavelengths only the ion pressure gradient is effective in driving the instability.

The modification of the line-bending stabilization ω_A^2 due to the shear-Alfven-drift wave coupling is found from Eq. (64) to be given by

$$\omega_A^2 \to \omega_A^2/F(k,\beta,\eta_i\gamma_m) \tag{70}$$

where

$$F(k,\beta,\eta_i\gamma_m) = 1 + \frac{\omega_A^2 k^2}{\gamma_m^2 - \frac{k^2}{2}(1+\eta_i)(2+\eta_i) + ik(2+\eta_i)\left[\gamma_m^2 - \frac{k^2}{4}(1+\eta_i)^2\right]^{1/2}}$$

For long wavelengths $k(1+\eta_i)<<2\gamma_m$, F(k) reduces to

$$F(k) \simeq 1+\omega_A^2 k^2/\gamma_m^2 .$$

Again the kinetic modification is small for $k<(\beta/\beta_c)^{1/2}$ and $\omega_A^2 \to \omega_A^2/2$ for $k=k_c=(\beta/\beta_c)^{1/2} < 1$. For $k >> k_c = (\beta/\beta_c)^{1/2}$ the line bending contribution is negligible.

(iii) High Plasma Beta

For $\beta>>\beta_c$ where $\omega_A<<\gamma_m$ the dispersion relation factors into two quadratic equations. One quadratic is Eq. (53) giving the MHD oscillations with $\alpha=1$, and the other quadratic is $\omega(\omega-k)-k^2\omega_A^2 = 0$ with the roots $\omega \cong -\omega_A^2 k$ and $\omega \cong k(1+\omega_A^2)$ with $\alpha>>1$.

B. Numerical Results

The electromagnetic dispersion relation from system (36)-(38) is

$$\det M = D(\omega, k, \varepsilon_n, \eta_i, \eta_e, \beta, T_e/T_i, q) = 0$$

$$= adf+2bce-ae^2-b^2f-c^2d \qquad (71)$$

and contains more physical processes than usually analyzed in low frequency stability theory. We attempt to describe the physics contained in Eq. (71) by first analyzing the limiting cases of electrostatic modes $a(k,\omega) = 0$, electrostatic-compressional mode coupling $af=c^2$, and then the fully electromagnetic modes. The six dimensionless parameters that determine the dispersion curve $\omega_\alpha=\omega_\alpha(k)$ are defined in Eq. (55). Clearly only a small range of variations around a set of reference values for these six parameters can be discussed. For reference values we take ε_n=0.25, q=2, η_i=η_e=2, T_e/T_i=1 and β_e=0.01. Some characteristic values defined in Secs. III and IV.B are ω_s=0.125, ω_A=1.77, γ_o=1.2, γ_m=1.7, β_c=0.021 and ε_p=0.08.

In the following numerical analysis we neglect the coupling to the sound waves. Thus the roots that tend to $\omega = 0$ as $k \to 0$ become invalid for $|\omega| \leqslant \omega_s$.

(i) Electrostatic Modes

The electrostatic modes are given by

$$a(k,\omega) = -1-\tau+\tau P(k,\omega,\varepsilon_n,\eta_i,\beta)|_{\beta=0} = 0$$

for $\omega^2 \gg \omega_s^2$, and are shown in Fig. 1 for τ=1 and ε_n=0.25. The modes have a threshold in ε_n and η_i which is analyzed in Terry et al.[12] The threshold for instability in the η_i ε_n plane is shown in Fig. 2 which gives the maximum $\gamma(k)=\gamma_m$ as a function of ε_n and η_i. Near threshold only the range of wavenumbers satisfying $|u_k| \leqslant \gamma_o$ is unstable as given by Eq. (65) with α=0. For η_i>2 all k are unstable with the maximum growth rate occurring near k=0.5.

The azimuthal phase velocity of the unstable electrostatic modes is small $\omega/k=u_k/2$ compared with the ion diamagnetic drift velocity $\omega/k=-(1+\eta_i)/\tau$. The low phase velocity leads to stochastic mixing of the ion trajectories at a small amplitude of the drift waves.[13]

Now, we consider the effect of increasing β within the context of the electrostatic polarization $a(k,\omega)\varphi$=0. The effect of increasing β is to decrease the ion grad-B drift velocity as given by Eq. (51). For $\beta_e \gtrsim 2\varepsilon_n/[1+\eta_e+(1+\eta_i)/\tau]$ the ion grad-B reverses the direction of the drift velocity from the ion diamagnetic direction to the electron diamagnetic direction.

The stabilizing effect on γ_k^{es} of increasing β is shown in Fig. 3 where we see that for $\beta \gtrsim 0.25$ the system is essentially stable to all k due to the large favorable ∇B drift.

In the following subsection (ii) we see how this stabilizing effect is cancelled by the compressional coupling of δB to φ.

(ii) Electrostatic-Compressional Coupling

Now we consider the effects of the coupling of the compressional component δB to the electrostatic component. Physically, the coupling arises from the convection of the pressure $dp/dt \cong 0$ producing a change in B due to the plasma diamagnetism as given in Eq. (56).

In Fig. 4 we show the growth rate $\gamma_k(\beta)$ obtained from the dispersion relation $af=c^2$ (Eqs. (36) and (38) with $\psi=0$) for the same parameters taken in Fig. 3. The stabilizing effect of β given by electrostatic polarization model, is weakened by δB. The system remains unstable for essentially all β. The maximum growth rate is slowly decreasing with increasing beta. The fluid expansion of the drift frequency denominators shows that the apparent stabilization due to $\omega_{\nabla B}$ in the electrostatic dispersion is cancelled by the δB coupling when the equilibrium conditions (51) are taken into account.

The dispersion relation $af=c^2$ neglects the coupling to the Alfven wave $\omega^2 \cong \omega_A^2$. For sufficiently large q (flute-like modes) this approximation is valid. For typical high β tokamak parameters, however, the coupling of $\omega(k)$ to ω_A is important.

(iii) Electrostatic–Shear Alfven Coupling

In the model often used for electromagnetic corrections to drift modes the coupling to the compressional mode is neglected, $\delta B=0$. The dispersion relation then reduces to $ad=b^2$. The stability for the references parameters is shown in Fig. 5a. We see the rapid increase of the growth rate with increasing β. For $\eta_i=\eta_e=0$ the $\gamma(k,\beta/\beta_c)$ is shown in Fig. 5b where now the system is stable for $\beta<\beta_c$ and MHD–like unstable for $\beta>\beta_c$. For $\eta_i \gtrsim 1$ there is no stable region as shown in Fig. 5a.

(iv) Full Electromagnetic Dispersion Relation

The electromagnetic dispersion relation det(M)=0 adds the coupling to the shear Alfven wave $\omega_A=k_\parallel v_A = (2/\beta_e)^{1/2}(\varepsilon_n/q)$. For $\beta \ll \beta_c$ given in Eq. (62) the frequency ω_A is well above the frequencies of the unstable pressure gradient driven modes, and the effect of the coupling is weak with $\alpha=\psi/\varphi\simeq-b/d\ll 1$. The small value of α prevents the convection of the electron pressure so that the growth rate varies with $\gamma_o=[2\varepsilon_n(1+\eta_i)]^{1/2}$ as shown in Figs. 1 and 2, where γ_k is independent of η_e.

For $\beta \lesssim \beta_c$ the ψ polarization becomes important. As β approaches β_c the polarization becomes MHD-like with $\alpha_k=1$ as given in Eq. (61). In the $\alpha_k \lesssim 1$ regime the electron pressure is also convected by the plasma motion, and the growth rate becomes $\gamma_m=\{2\varepsilon_n[(1+\eta_i)/\tau+(1+\eta_e)]\}^{1/2}$.

For small k the polarization α_k, Eq. (61), remains MHD–like even for $\beta<\beta_c$ and for these long wavelength modes the stabilization from line bending, Eq. (70), is effective and gives rise to the classical FLR dispersion relation, Eq. (54). For $k>k_c=(\beta/\beta_c)^{1/2}$, as discussed following Eq. (62), the field line bending effect is weak.

In Fig. 6 we show the results comparable to those in Figs. 3,4 and 5 now derived for the full electromagnetic dispersion relation. Introducing the coupling to the shear Alfven waves adds two branches to the dispersion relation. The appropriate fluid limit of the dispersion relation is the fourth order polynomial in ω derived in Ref. 1 and given appropriately in Eq. (64).

In Fig. 7 we show the results given by the fluid approximation as β/β_c increases through unity. In Fig. 8 we show for the same parameters as in Fig. 7 the results obtained from the kinetic dispersion relation. Both the fluid and the kinetic theory show the transition from microturbulence to macroturbulence, as reported by Horton et al.[1] from fluid theory. The transition occurs with the shift of the maximum growth rate from $k=k_\vartheta\rho\sim\frac{1}{2}$ to $k_\vartheta\rho=0$ as β/β_c increases through unity. The magnitude of the maximum growth rate γ_m increases modestly during the transition.

The principal kinetic effects on the pressure gradient driven modes are seen by comparing Figs. 7 and 8. With kinetic theory the unstable spectrum of k is broader, and the maximum growth rate is significantly reduced. The strength of this reduction in γ_m is a strong function of ε_n. The fluid growth rate arises from an asymptotic expansion of $(\omega-\omega_D)^{-1}$ in powers of $k\varepsilon_n/\omega$. For a typical pressure gradient mode $\omega/k\sim\varepsilon_n^{1/2}$, and thus the asymptotic expansion parameter varies as $\varepsilon_n^{1/2}$. For $\varepsilon_n \leqslant 0.05$ the fluid expansion becomes quantitatively accurate as shown in Fig. (4) of Terry et al.[12] For $\varepsilon_n \gtrsim 0.1$, however, the fluid expansion is only in qualitative agreement with the kinetic growth rate as evident from comparing Fig. 7 with Fig. 8. (or Fig. 3 of Terry et al.[12]).

V. Summary and Conclusions

The full kinetic electromagnetic dispersion relation is derived and analyzed for density-temperature gradient driven instabilities in regions of unfavorable magnetic curvature. Instabilities due to dissipative trapped electrons and passing electron Landau resonances are eliminated by taking the electron response as real in the limit $\omega \ll \omega_{be}$. All finite Larmor radius effects from the ion Bessel functions and the full ion drift resonance effects are retained in the ion response functions. The response functions are computed by using the guiding center dispersion function (GCDF) routines given by Similon et al.[6]

The electrostatic limit (ES) and the MHD limit of the dispersion relation det(M)=0 are well known. In the fluid limit both the ES and MHD mode equations are quadratic equations in ω with sharp thresholds of instability given by the vanishing of their discriminants. The growth rate in the ES limit varies with $\gamma_o=[2\varepsilon_n(1+\eta_i)]^{1/2}$ arising from the ion pressure gradient and in the MHD limit varies with $\gamma_m=\{2\varepsilon_n[(1+\eta_e)+(1+\eta_i)/\tau]\}^{1/2}$ arising from the total pressure gradient. In the ES limit the electron fluctuation is not E×B convected but given by $\delta p_e=T_e\delta n_e \simeq p_e(e\varphi/T_e)$ from the parallel electron momentum balance.

In Sec. IV we derive formulas for the transitional dispersion relation for the variation of γ_k and the critical wavenumber $k_m(\varepsilon_n,\eta_i,\beta,q)$ that maximizes the growth γ_k over k. We show that as β approaches the critical beta β_c from below, the maximum of the growth rate shifts from $k_\vartheta\rho$ finite to $k_\vartheta\rho \to 0$. For $\beta \lesssim \beta_c$ the long wavelength part of the unstable spectrum is MHD polarized while the short wavelength part $k_\vartheta\rho > (\beta/\beta_c)^{1/2}$ remains electrostatic.

The same qualitative features of the transition in the form of instabiltiy with β/β_c are given by the fluid limit of the dispersion relation as reported by Horton et al.[1] The kinetic theory spreads out the transitional behavior from that predicted by the fluid approximation. The additional dispersion in the stability criterion arise from strong broadening of the guiding center response functions at finite ε_n. The fluid limit is an asymptotic expansion in small $\omega_D/\omega \sim k\varepsilon_n/\omega \sim \varepsilon_n^{1/2}$ which is quantitatively accurate only for $\varepsilon_n \lesssim 0.05$.

The physical picture of instability given by the kinetic-electromagnetic theory is that for typical tokamak parameters the plasma is unstable at all values of β. For low β/β_c the dominant instability is confined to short wavelengths that scale with the ion gyroradius or the ion inertial scale length $\rho = c(m_i T_e)^{1/2}/eB$. The measure of particle diffusion is the drift wave diffusion coefficient $D_{d\omega} = \gamma_m/k_m^2 \cong (\rho/r_n)(\frac{cT_e}{eB})$. As β/β_c increases there is a continuous change in the stability parameters and a weaker enhancement of the growth rate. The scale of the dominant instability, however, increases as $\rho/(1-\beta/\beta_c)^{1/2}$ given by Eq. (66). For $\beta \to \beta_c$ the dominant wavelength diverges on the kinetic scale of ρ and the dominant wavelengths become global. Although the stability parameter γ_k varies contiuously with $\varepsilon_n, \beta, \eta_i, \eta_e, q, \tau$, the change of scale at β_c appears to produce a discontinuous change in the thermodynamic quantities such as the particle diffusion and the thermal conductivity of the plasma. The nature of this type of effective phase transition requires further study.

From this point of view, derived from the kinetic stability theory, the MHD stability criterion <u>does</u> <u>not</u> determine the threshold of instability. The plasma is essentially always unstable even for β well below β_c. Instead the MHD stability threshold determines the threshold for global or macroscopic instability. This interpretation implies a continuous change in the microscale fluctuations observed, for example, by microwave scattering experiments, but an abrupt onset of thermal energy loss with the onsetof low m MHD polarized motions at certain critical values of β/β_c.

Acknowledgements

The work was supported by the DOE Contract #DE–FG05–80ET–53088 and by the Korea Advanced Institute of Science and Technology.

References

1. W. Horton, D. I. Choi and B. G. Hong, Phys. Fluids. 26, 1461 (1983).

2. C. Z. Cheng, Phys. Fluids 25, 1020 (1982).

3. K. Itoh, S. I. Itoh, S. Tokuda and T. Tuda, Nucl. Fusion 22, 1031 (1982).

4. G. Rewoldt, W. M. Tang and M. S. Chance, Phys. Fluids 25, 480 (1982).

5. D. E. Hastings and J. E. McCune, Phys. Fluids 25, 509 (1982).

6. P. Similon, J. E. Sedlak, D. Stotler, H. L. Berk, W. Horton, and D. Choi, "Journ. Comp. Phys. 54, 260 (1984).

7. T. M. Antonsen and B. Lane, Phys. Fluids 23, 1205 (1980), and T. M. Antonsen, B. Lane and J. J. Ramos, Phys. Fluids 24, 1465 (1981).

8. W. M. Tang, J. W. Connor and R. J. Hastie, Nucl. Fusion 20 1439 (1980).

9. W. Horton, R. D. Estes and D. Biskamp, Plasma Phys. 22, 663 (1980).

10. W. Horton, D. I. Choi and W. M. Tang, Phys. Fluids 24, 1077 (1981).

11. D. Brock and W. Horton, Phys. Fluids 24, 271 (1982).

12. P. Terry, W. Anderson and W. Horton, Nucl. Fusion 22, 487 (1982).

13. W. Horton, Plasma Physics 23, 1107 (1981).

Figure Captions

1. The unstable modes in the electrostatic approximation $a(k,\omega) = 0$ for $\tau=1$ and $\varepsilon_n=0.25$ and varying $\eta_i=1,2,3$ with $\beta=0$.
2. The electrostatic growth rate maximized over k as a function of η_i and ε_n at $\beta=0$.
3. The growth rate showing the stabilizing effect of finite β in the grad B drift within the purely electrostatic polarization $a(k,\omega)=0$ approximation, with $\tau=1$, $\varepsilon_n=0.25$, $\eta_i=2$.
4. The growth derived from the $\varphi-\delta B$ coupling neglecting the shear Alfven coupling. The parameters are the same as in Fig. 3.
5. The growth rate γ as a function of $k_\vartheta\rho$ and β/β_c for the $\varphi-\psi$ coupling with $\delta B=0$. Fig. 5a shows instability for $\eta_i=\eta_e=2$ for all β/β_c whereas Fig. 5b, with $\eta_i=\eta_e=0$, shows the instability only for $\beta\geqslant\beta_c$ giving the MHD threshold condition.
6. The growth rate derived from the full electromagnetic dispersion relation det M=0 for the parameters used in Figs. 3 , 4 and 5. The change from Fig. 4 is due to coupling with the shear Alfven waves which adds two branches to the dispersion relation.
7. The transition from micro to macroinstability with β/β_c passing through unity as predicted by the fluid approximation.
8. The same transition given in Fig. 7 computed here from the kinetic-electromagnetic dispersion relation.

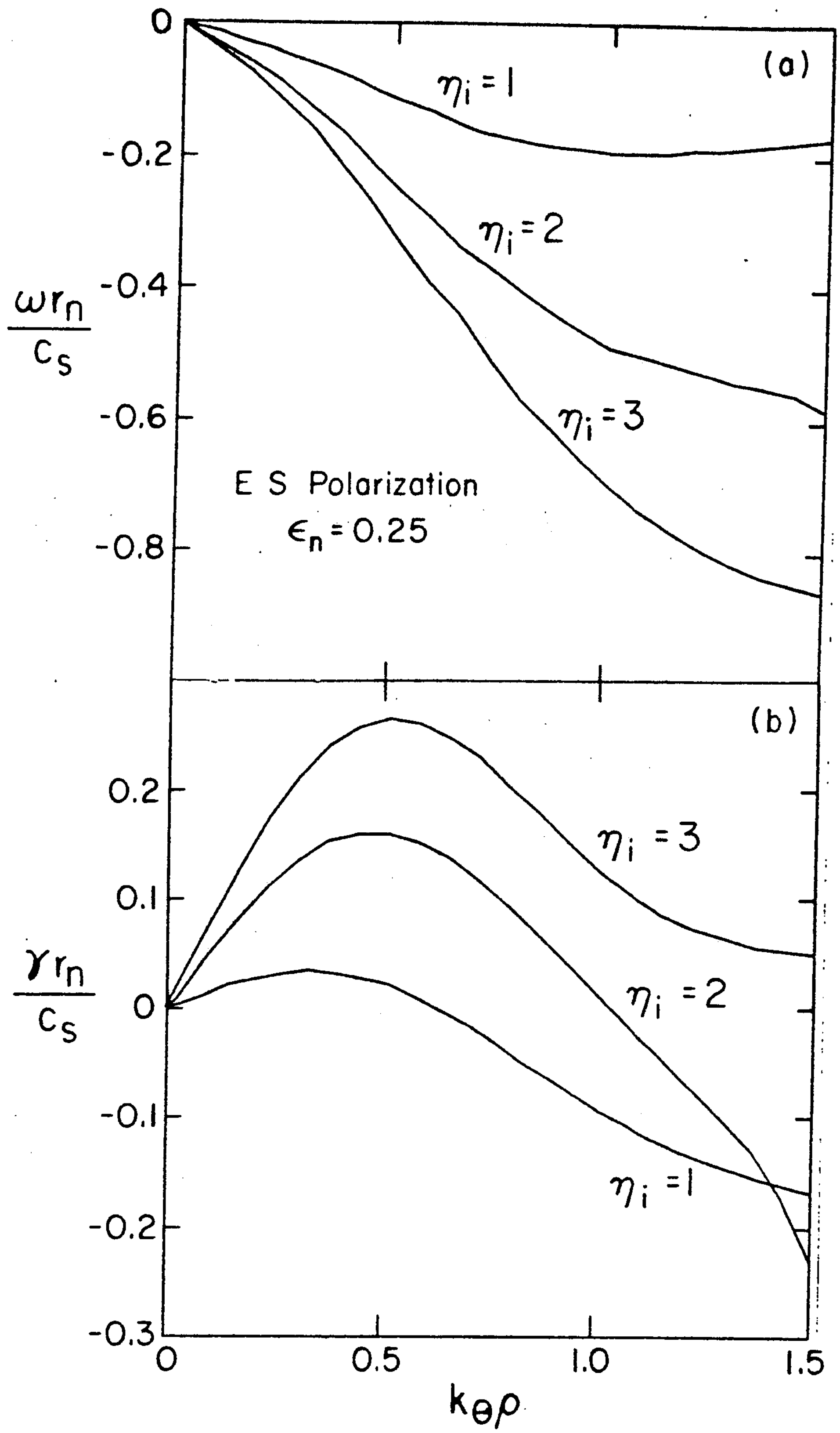

(a)
$\eta_i = 1$
$\eta_i = 2$
$\eta_i = 3$
E S Polarization
$\epsilon_n = 0.25$
$\frac{\omega r_n}{c_s}$
0
-0.2
-0.4
-0.6
-0.8
(b)
$\eta_i = 3$
$\eta_i = 2$
$\eta_i = 1$
$\frac{\gamma r_n}{c_s}$
0.2
0.1
0
-0.1
-0.2
-0.3
0
0.5
1.0
1.5
$k_\theta \rho$

FIG. 1

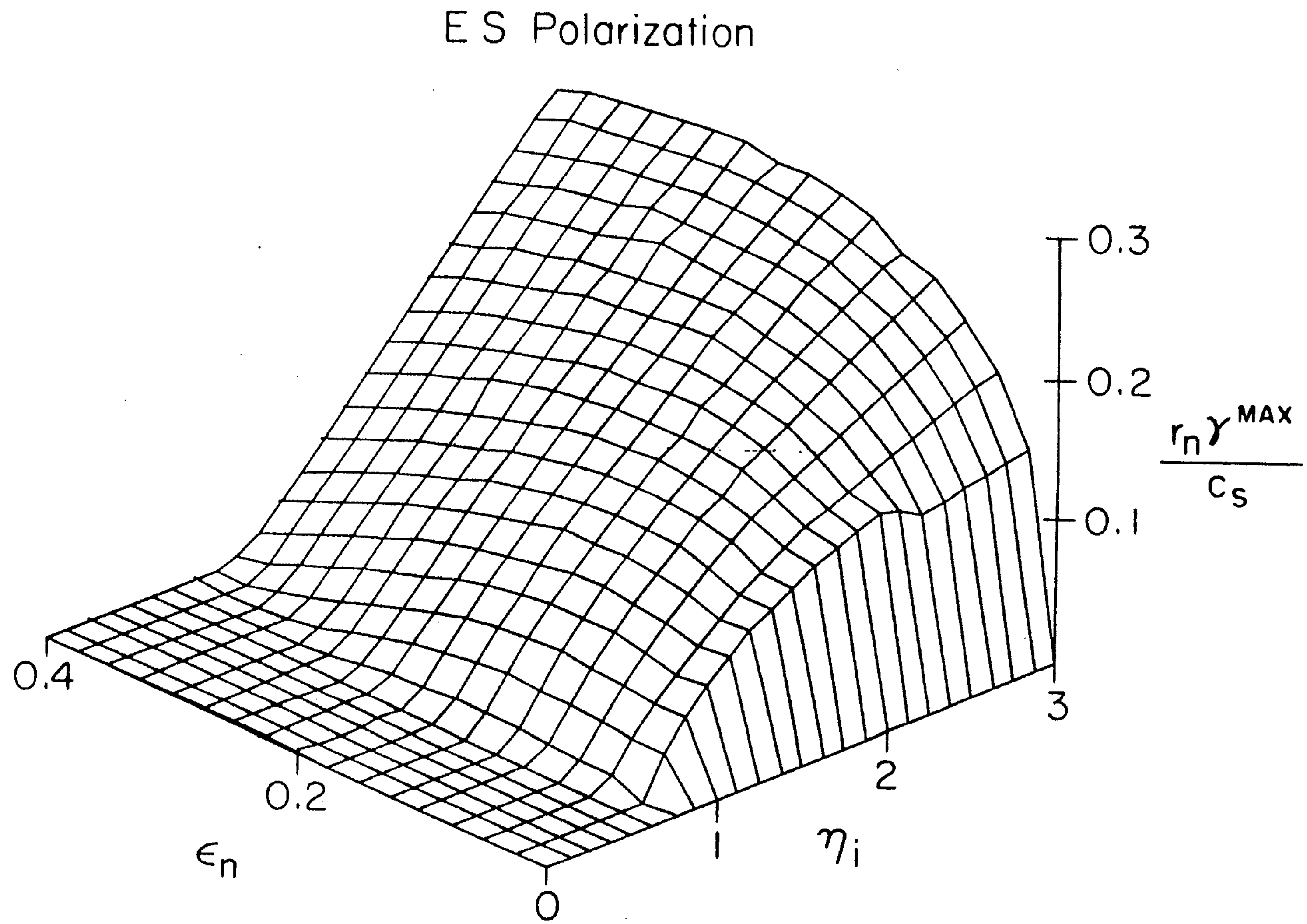
ES Polarization
0.4
0.2
0
ϵ_n
1
2
3
η_i
0.1
0.2
0.3
$\frac{r_n \gamma^{MAX}}{c_s}$

FIG. 2

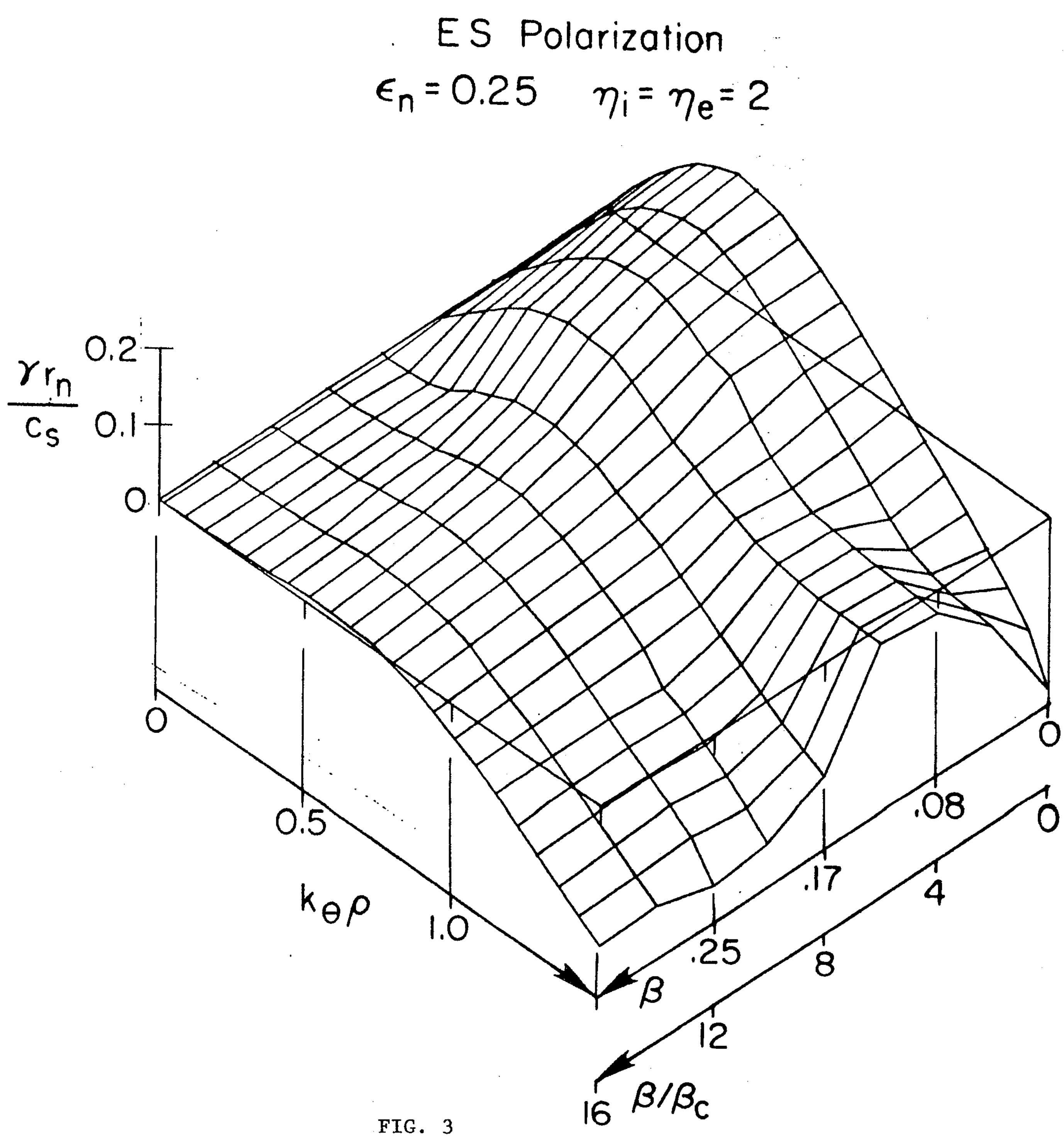

ES Polarization
$\epsilon_n = 0.25 \quad \eta_i = \eta_e = 2$
$\frac{\gamma r_n}{c_s}$
0.2
0.1
0
0
0.5
1.0
$k_\theta \rho$
β
.25
.17
.08
0
β/β_c
16
12
8
4
0

FIG. 3

$\phi - \delta B$ Coupling

$\epsilon_n = 0.25 \quad \eta_i = \eta_e = 2$

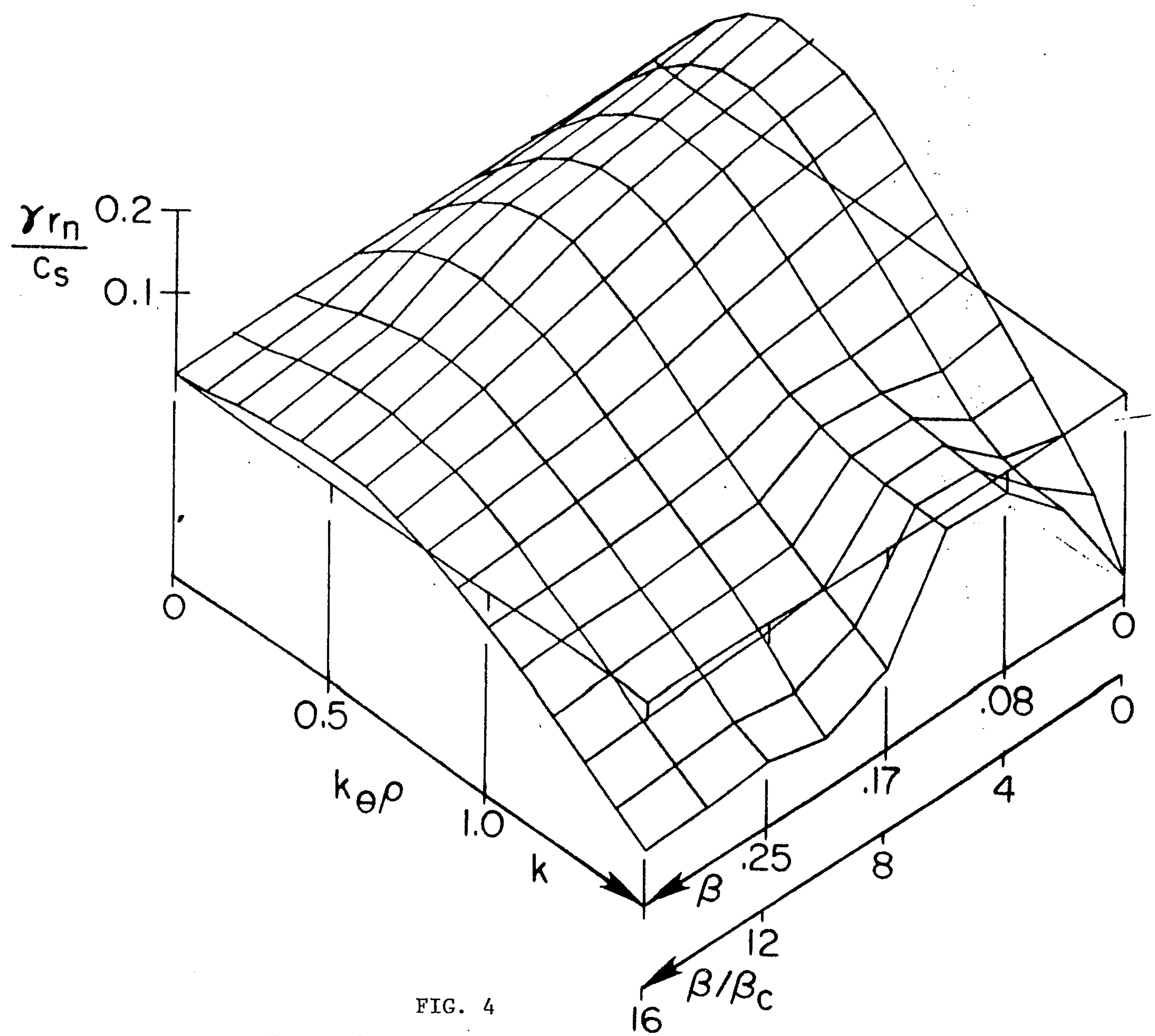

FIG. 4

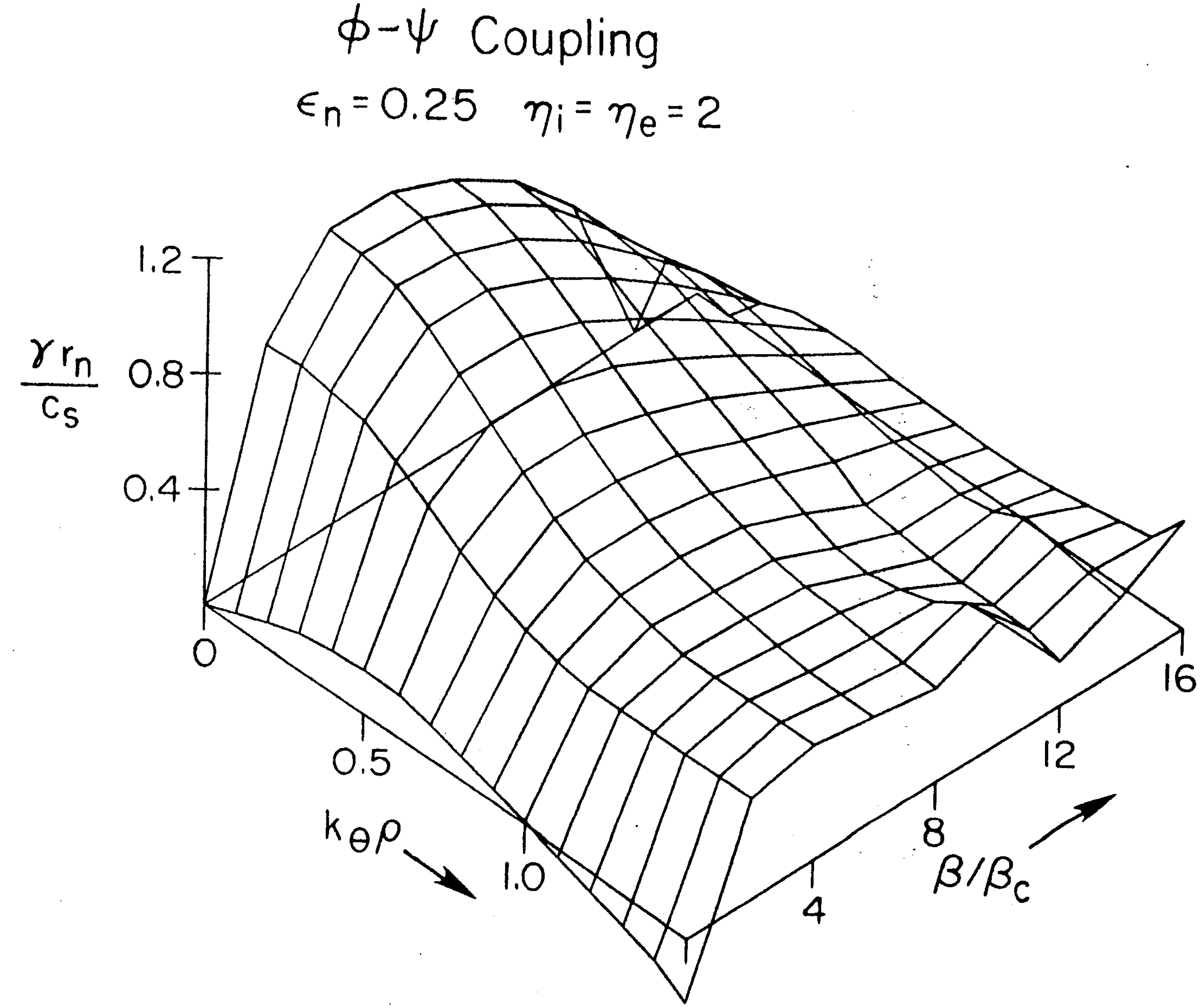

$\phi-\psi$ Coupling
$\epsilon_n = 0.25 \quad \eta_i = \eta_e = 2$
$\frac{\gamma r_n}{c_s}$
1.2
0.8
0.4
0
0.5
1.0
$k_\theta \rho$
4
8
12
16
β/β_c

FIG. 5a

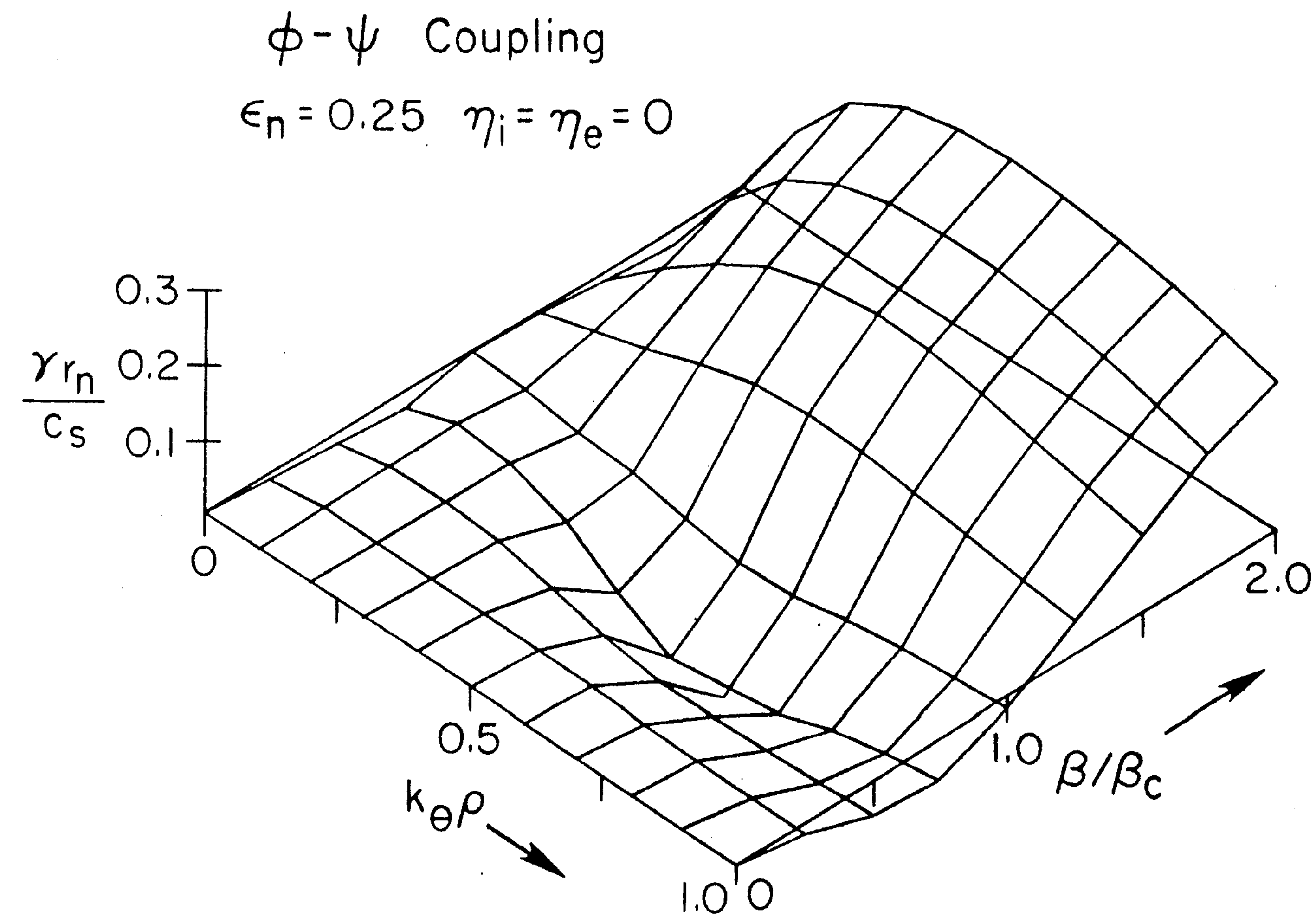

$\phi - \psi$ Coupling
$\epsilon_n = 0.25$ $\eta_i = \eta_e = 0$
$\frac{\gamma r_n}{c_s}$
0.3
0.2
0.1
0
0.5
1.0
$k_\theta \rho$
0
1.0
2.0
β/β_c

FIG. 5b

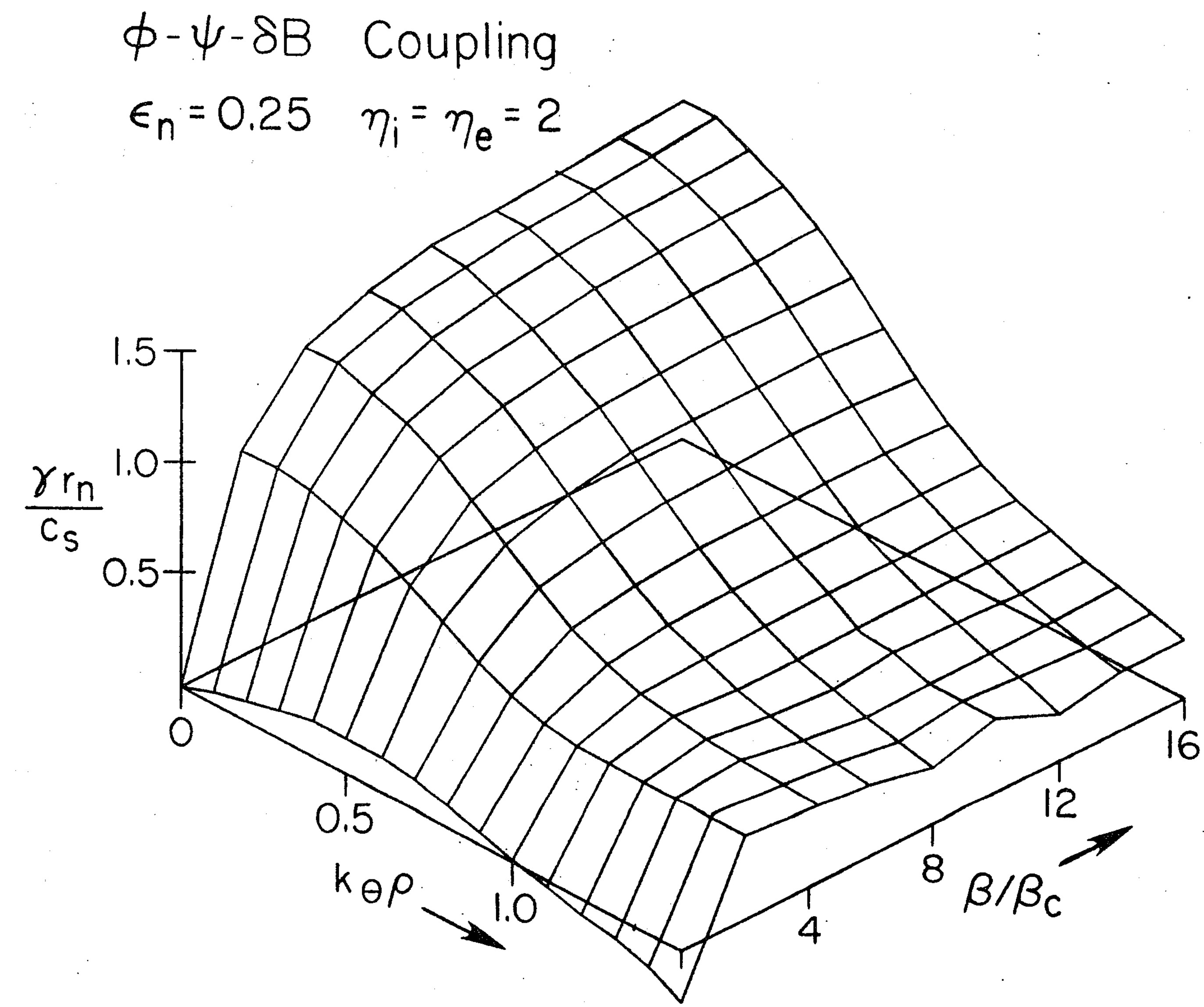

ϕ-ψ-δB Coupling
ϵn = 0.25 ηi = ηe = 2
1.5
1.0
0.5
γrn/cs
0
0.5
kθρ
1.0
4
8
12
16
β/βc

FIG. 6

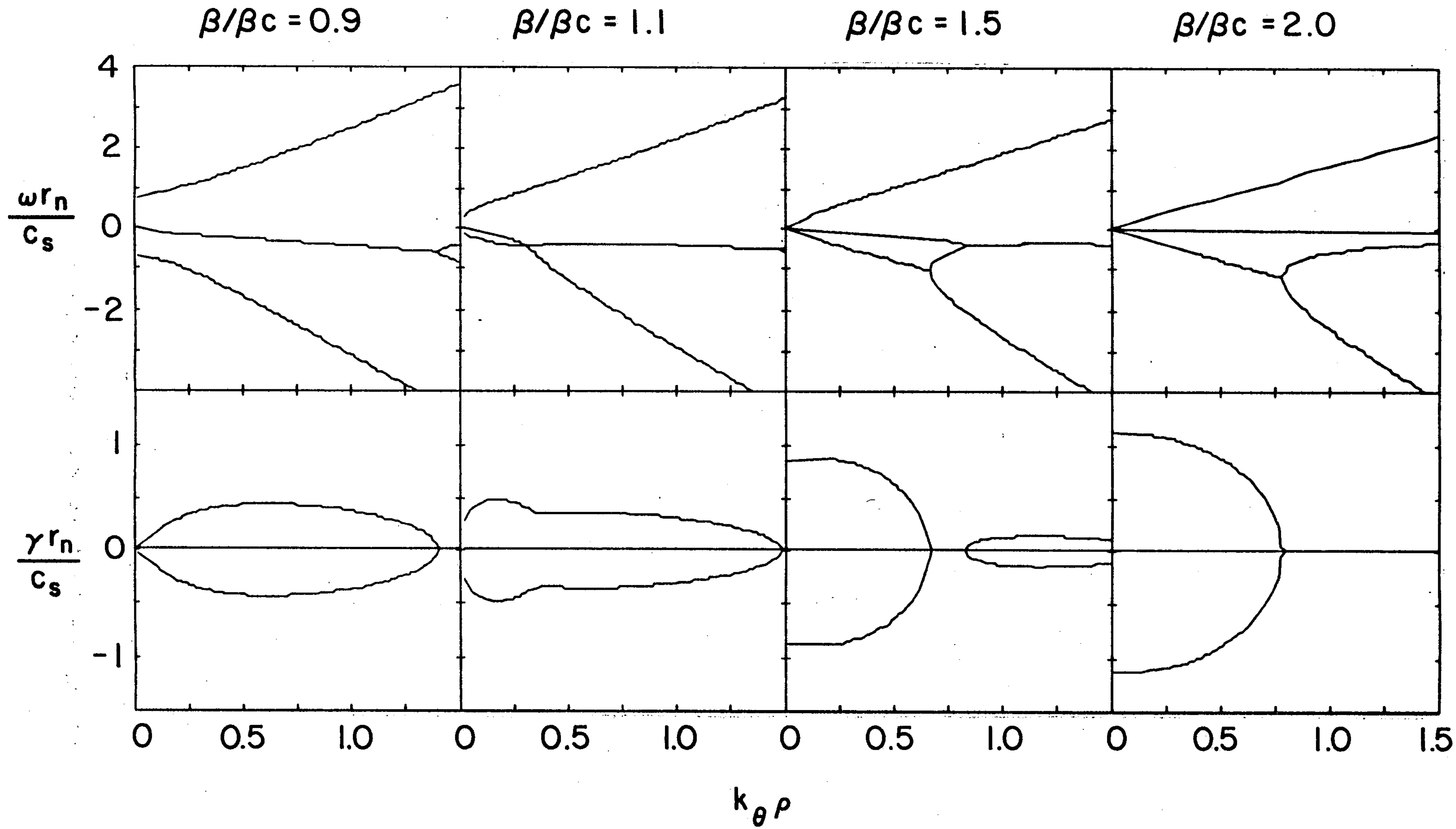

FIG. 7

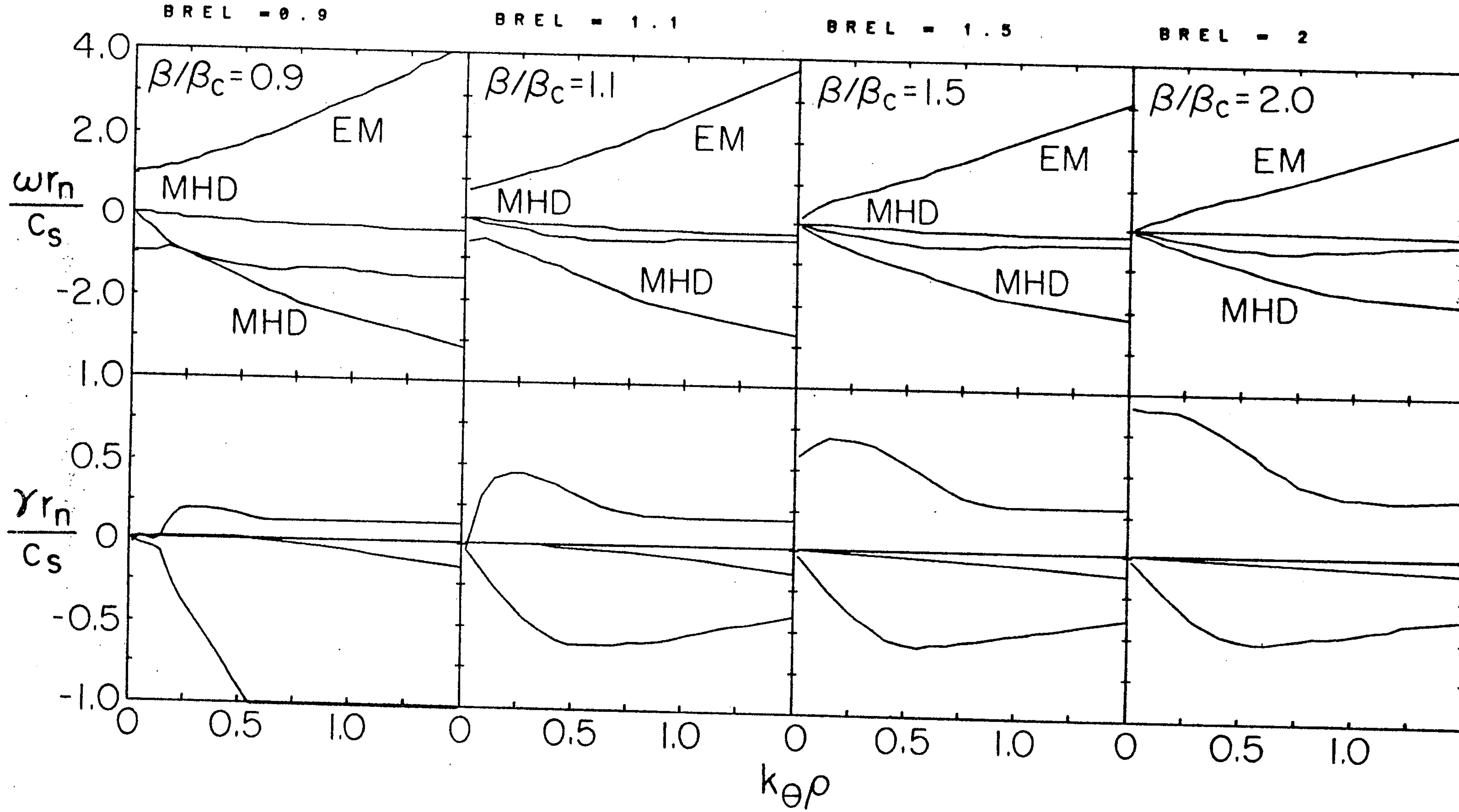
BREL =0.9
BREL = 1.1
BREL = 1.5
BREL = 2
β/β_c=0.9
β/β_c=1.1
β/β_c=1.5
β/β_c=2.0
EM
MHD
$\frac{\omega r_n}{c_s}$
$\frac{\gamma r_n}{c_s}$
$k_\theta\rho$

FIG. 8